

# A GIS-based Simulation and Visualization Tool for the Assessment of Gully Erosion Processes

Adel Omran (✉ [adel.omran@unipv.it](mailto:adel.omran@unipv.it))

Pavia University

Dietrich Schröder

Stuttgart University of Applied Sciences

Christian Sommer

Heidelberg Academy of Sciences and Humanities

Volker Hochschild

University of Tübingen

Michael Maerker

Pavia University

---

## Research Article

**Keywords:** Soil erosion, Gully simulation model, Python application, GIS, Visualization

**Posted Date:** June 22nd, 2022

**DOI:** <https://doi.org/10.21203/rs.3.rs-1751074/v1>

**License:**  This work is licensed under a Creative Commons Attribution 4.0 International License.

[Read Full License](#)

---

# Abstract

Gully erosion is known to affect soil productivity, limit land use, and to pose threats on infrastructure in many parts of the world. Gully erosion has been largely neglected because it is difficult to model and visualize its effects. Many gullies grow rapidly to large sizes, making effective control technically difficult and often too expensive. To assess the susceptibility of soils and substrates to gully erosion, the triggering factors must be identified and analyzed. For this study, a simulation of gully development over time was implemented in Python based on the topographic characteristics of the test watershed, soil properties, and measured runoff. The full simulation GIS was tested on a gully in the KwaThunzi region, South Africa. The results are very promising and allow a 2D/3D visualization of the time series of gully evolution.

## 1 Introduction

Soil erosion is recognized as a global environmental and agricultural issue threatening especially semi-arid areas such as in Australia, Russia, South Africa, Chile, Iran, and the Mediterranean Regions of Europe. It has been estimated that about 75 billion tons of soil per year are eroded by wind and water related processes often impacting agricultural land [5]. Soil erosion by water, such as gulying, is acknowledged as a global main driver of land degradation [27]. Gully erosion is typically defined as a deep channel that has been eroded by concentrated water flow, removing surface soils and materials [42]. Gullies are distinguished from rills based on a critical cross-sectional area that corresponds to the size of the channel that can no longer be erased by normal tillage operations [3, 8]. Gully erosion is related with a variety of on-site and off-site damages, particularly impacting agricultural areas. On-site damages include the direct loss of arable land resulting in significant soil losses, reduced soil fertility, loss of crops, and vegetation cover, as well as damages to infrastructure such as roads, power lines, and communication networks [15, 13, 14]. As an outcome of their high erosion rates, gullies enhance the connectivity of slope systems and lead to an increased sediment delivery. Estimates indicate that gullies are accountable for 20 to 80% of a catchment's mean sediment yield (e.g., [19, 46]). In particular, the produced sediments washed into the drainage network are related to off-site damages including the reduction of water quality within the adjacent river systems. Moreover, the gully-related sediments can be a transport medium for chemical, physical, and biological pollutants. This strongly impairs freshwater ecosystems and their ecosystem services (e.g. [16]) and leads to increased costs in physical, chemical, and biological water treatment in order to provide drinking water as well as water for industrial (e.g. cooling, hydropower) and agricultural use (irrigation) (e.g. [48]).

Even though gully erosion has a major quantitative impact on a catchment's sediment yield, (e.g., [20]), it is rarely taken into consideration by erosion models [8, 30, 46]. One main reason is the high spatial and temporal heterogeneity of gully erosion processes dynamics [40, 38]. For this reason, the mapping of gully erosion is relevant for the identification of hazards and, if necessary, initiation of soil conservation measures. Therefore, many studies discuss the occurrence, modeling, and prediction of gully erosion events (see [46]). The prediction and modeling of soil erosion is an important basis for decision-making

for soil conservation and landscape planning [9]. Due to the knowledge gain provided by simulation models, many models have been applied to map, simulate, and predict gully erosion processes as well as related geomorphic features.

In terms of assessing gully erosion quantitatively, different modeling approaches have been proposed. In general, the potential location of a gully can be identified with probabilistic models [21, 22, 1]. Empirical models offer an alternative approach by predicting retreat rates of a gully headcut erosion (e.g., [45, 30, 11, 18]). However, only a few studies focused on gully widening and depth erosion [2]. Moreover, empirical models are limited in terms of their predictive capacity. Consequently, there is a strong need for process-oriented models that are able to assess most of the gully-related processes, such as headcut retreat, gully-widening and gully-deepening.

Moreover, the approach should be simultaneously also sufficiently flexible to handle different spatio-temporal scales. This is even more essential for the assessment of both expected future climate and land use changes. Only a few models such as DIMGUL/STABGUL [37, 40, 38] are capable of simulating gully evolution dynamics. DIMGUL/STABGUL models allow the simulation of gully morphology considering the causes for their development. Hence, stable gully morphology can be predicted [49, 23], as well as the conditions supporting the incision of ephemeral gullies [29], gully head growth rate [43, 44], and the transformation of the length profile [36].

The process of gully formation needs a precipitation events, that lead to an infiltration surplus or saturation surplus and produces a water discharge that exceeds the runoff threshold required to remove and transport sediments. Additionally, topographic circumstances including slope, exposition and catchment area control the amount and volume of water runoff. Depth and morphology of the gully cross-section are dictated by soil erodibility as well as the lithostratigraphic characteristics of the area. Kosov et al. (1978) [17] explained the mechanism of the gully development dynamically and statically pointing out that there are two stages of gully development leading to two types of gully erosion models: 1) the dynamic model predicting rapid changes of gully morphology in the first stage of gully development covering only ca. 5% of the entire gully lifetime; 2) the static model that calculates the final morphometric parameters of stable gullies covering the rest of the gully lifetime (see also [37]). Hence, the two models are used to predict both the development of gullies and their final morphologies.

Traditionally, the modeling of gully and channel erosion in GIS environments raised issues related to computing capacity and efficiency, specific input data requests, and inflexible programming interfaces. Generally, GIS is acknowledged as a versatile tool for the analysis and visualization of model results, incorporates sophisticated statistical analytical tools and offers computational solutions for model calibration and validation [32, 24]. Recently GIS is becoming increasingly relevant for spatial environmental modelling and specifically for gully modelling, as it offers Application Programming Interfaces (API) and supports script languages such as Python, and libraries for raster algebra. A model that has been implemented in a GIS environment can be used as a tool within the user interface and the input and output is stored in standardized geodatasets, so there is no need for transformation between

different, model-specific formats. Further advantages for such mode development include customizable development tools, integration of built-in raster calculators [47] and visual programming languages.

The objective of this study is to simulate processes of gully incision and thus, to estimate the gully evolution over longer time periods using a Python-based tool integrated in a GIS-environment. This simulation is based on the gully models proposed by Sidorchuk (1998, 1999, 2003) [41, 37, 40] and was originally provided in the form of a Fortran code. Sidorchuk's models allow the simulation of the gully evolution considering different lifetime stages (see above). The main aim for this work is to simulate gully erosion in 2D and 3D within a GIS-environment, either using a commercial or an open-source GIS-environment. The GIS-based gully erosion model was set up and run based on a study area located in KwaZulu-Natal, South Africa characterized by large gully systems developed in colluvial material also called Masotcheni formation [6]. Subsequently, the simulation results were compared with the existing gully morphology. Finally, the gully model modelling framework allows also the reconstruction of the initial environmental conditions before gully incision.

## 2 The Dimgul Theoretical Framework

Gully formation originates under certain conditions when the force of the water flow exceeds a certain threshold value, and the shallow water flow begins to concentrate along flow lines. Particularly, these thresholds are reached at knickpoints or at depressions along the slope. Several flow lines may merge and increase the probability for gully development, eventually merging the knickpoints and forming a single incised stream [12]. Then the gully form progresses via headwall migration and the channel widens.

As described by [37] the first phase of gully initiation is intense and characterized by the instability of morphological characteristics like volume, area, length, width and depth. Instead, the last stage describing the stable gully evolution is associated with sediment mobilization and deposition at the gully bottom. Moreover, lateral widening and mass movements of the gully side walls are observed. Empirical measurements by [17] demonstrate that the first stage evolves rapidly in the first 5% of the gully's lifetime, but accounts for 60% of its area and 35% of its volume. In the remaining lifetime gully area and volume are still subject to change, but under more stable conditions (Fig. 1).

Sidorchuk's model of gully erosion considers the following fundamental processes during the dynamic initial stage: Water flow induced by substantial precipitation events excavates a rectangular channel in the upper soil. Destabilization of the vertical incision walls triggers shallow mass movements and transform the rectangular cross-section to a trapezoidal form during the time period between relevant precipitation events. The gully erosion rate is affected by multiple factors including surface runoff flow velocity, incision depth, turbulence of water flow, air and water temperature, soil texture, soil mechanical characteristics and the influence of a protective vegetation cover.

$$\frac{\partial Z}{\partial t} - a \frac{dZ}{dx} = 0 \text{ transport equation (Eq. 1)}$$

With

$$a = k_E H \frac{Q}{W} \text{ (Eq. 2)}$$

Where,

$k_E$  = longitudinal erosion coefficient

$W$  = flow width

$Q$  = water discharge

$H$  is 1 when flow velocity  $U$  is more than critical velocity of erosion initiation  $U_{cr}$  and  $H = 0$  when  $U \leq U_{cr}$

The complex interaction between flow and soil cohesiveness in the gully section is modeled with a rather simple transport calculation given by Eq. 1 for bed elevations  $Z$  along the main flow line in direction  $x$ . This transport equation (Eq. 1) considers the feedback phenomenon of the relief transformation on the erosion rate and it takes into account a rather limited number of input characteristics such as the initial longitudinal profile for each flow line, the specific water discharge distribution along this line, the erosion coefficient  $k_E$  and the associated critical velocity of erosion initiation for each soil texture (Eq. 2).

### 3 Study Area And Environmental Data

The model framework described above was tested in the Drakensberg Foothills situated in the KwaZulu-Natal Province of South Africa. Following the geomorphic classification by Partridge et al. (2010) [28] the area belongs to the Eastern Coastal Hinterland with a Cwb climate following the Koeppen-Geiger classification, which is characterized by a warm temperate climate, with warm summers and dry winters [10]. At the close-by Himeville climate station, monthly mean temperatures range between 7 and 19°C and mean annual rainfall amounts to 935 mm mainly falling in the austral hemisphere's summer months [25]. The KwaThunzi Gully (Lat - 29.6164°, Lon 29.6480°) is located at an elevation of ~ 1200 m a.s.l. on a slope exposed to southwest covered by grassland in the upstream area of the Mkomazi River (Fig. 2). The gully developed in colluvial sediments of the Masotcheni formation that is of Late Pleistocene age [7, 6]. The underlying basement belongs to the Beaufort Group shale stones that is disturbed by a network of dolerite dykes in turn forming the local erosion bases. The gully walls expose a sequence of paleosols and colluvial deposits of the Masotcheni formation up to a thickness of 9 m comprising a basal unstratified layer, followed upwards by a transitional layer and several paleosols with columnar structures, iron-manganese and carbonate concretions, as well as leaching zones. The overlying recent Solonetzic soil is developed to a thickness of 30 cm characterized by a columnar structure and a Clay-Loam texture (USDA: ClLo).

The main model input data comprise: 1) the terrain morphology (digital elevation model); 2) the soil and lithological composition (substrate and soil mechanic parameters), and 3) meteorological

measurements. The topographic data, in terms of a digital elevation model (DEM) of the KwaThunzi gully, was created using a structure-from-motion approach. The images were acquired in the field on January 13, 2018 by a UAV equipped with a Canon PowerShot S110 camera. For the 3D processing the Mavis (v.17.09.00) software by BitMapping was used. Initially, the camera images were matched with their GPS-coordinates based on the time tag in both datasets. Subsequently, images exceeding a maximum threshold in yaw, pitch, or roll were excluded. This allowed the alignment of images and tie-point generation. The majority of images overlap with at least 10 neighboring images. Subsequently, a gridded DEM has been generated with a resolution of 10 cm and a RGB orthomosaic that features a spatial resolution of 5.5 cm. The DEM was resampled to a spatial resolution of 1 m.

Surface runoff data have been derived from discharge measurements at a gauging station close to the study area at Lundy's Hill (Lat - 29.9098°, Lon 29.7398°) with a data time series of more than 60 years. The lithology and substrates were investigated in the field using selected sections that were chosen based on the geological map (see [6]). The lithological section of the study area was finally classified into four soil/substrate units which are, topsoil, paleosol, transitional colluvial layer, and the colluvial base layer. The main soil parameters that are used in the model are calculated for each layer such as: i) critical velocity values following Bogomolov & Mikhaylov (1972) [4] ii) stable slope that was determined in radians for each unit, and iii) the erodibility coefficient (K) after (Renard,1997) [33].

## 4 Methodology

Implementing the gully erosion model in a GIS system is quite complex and involves the conceptualization of a workflow that includes the following steps: 1) processing of input data, 2) model calculation, 3) analysis, and 4) visualization of results. The workflow is then implemented using a visual programming tool that is integrated in GIS (model builders). We used python as programming language that supports fully automated simulations [34]. Complex physically-based models such as the chosen gully models usually are based on partial differential equation solutions. However, these equations can be fully implemented in a GIS framework using the system's geospatial data management application programming interface (API).

The rate of gully incision is controlled by water flow velocity, channel depth, as well as by soil texture, soil mechanical pattern, and the degree of protection by vegetation [37]. Based on the elevation and distance of specific points from the gully mouth along the longitudinal profile of the flow line (including existing gullies) the gully morphology is calculated.

Therefore, also the change in water discharge over time was estimated for all these points using surface specific runoff derived from the discharge data available at Lundies Hill. The empirical relationships (see Eqs. 1 and 2) are used to calculate flow width, flow depth, and flow velocity. Soil or substrate properties are used in the model comprising critical velocity, slope stability, and erodibility coefficient as described above.

The complete simulation can be divided into four main steps (Fig. 3): 1) identification and delineation of the flow path network from the digital elevation model (DEM), 2) preparation of the topographic data in terms of selecting the flow path that is representing the main stream flows of the gully, 3) calculation of the main parameters characterizing the resulting gully morphology such as length, width, depth, and volume for different time steps (e.g. yearly time step), and 4) creation of 2D and 3D representations of gully erosion for the established time period.

## 4.1 Flow path extraction

The aim of this step is to extract the flow line paths from the digital elevation model. Therefore, the concept of Strahler's stream ordering technique was applied to perform a qualitative and quantitative assessment of the drainage system. The flow lines can be extracted in a GIS-environment using a specific automated tool for ordering, rasterization and vectorization flow lines [35, 26]. This tool is organized in the following steps as illustrated in Fig. 4: 1) Creation of a DEM (if not available for analysis), 2) Application of a fill sink procedure to preprocess the DEM, 3) calculation of local flow directions, 4) calculation of flow accumulation, 5) Selection of the optimum threshold value for stream line extraction, 6) Rasterization of flow lines based on a Strahler order segmentation and 7) vectorization of the flow lines.

## 4.2 Derivation of topographic input information

In the second step the required topographic data is prepared that is used in the model simulation step. The topographic files contain the elevation data along the flow lines at discretized points as well as the corresponding values of the flow accumulation that are extracted in the first step together with the thickness of each soil/substrate layer measured in the field. Additionally, a file containing the global coordinates of each segmentation point along the selected flow line is generated including latitude (x), longitude (y), and elevation (z) for each point. The model uses Esri's ArcGIS Model Builder, including several customized Python tools as shown in Fig. 5.

For the elevation data of each layer along the flow line, two digital elevation models were used. The first DEM represents the initial situation of the area before gully erosion starts and the second DEM which reflects the situation of the study area after gully erosion, or at a specific time step during gully evolution. The initial DEM can be reconstructed by re-filling the gully trench using the fill module applied on the present-day DEM of the study area or creating an initial DEM e.g. from stereo aerial photos with high resolution. For the data preparation, we implemented two Python scripts within full ModelBuilder including different tools. The first part of the model discretized the selected flow line into point geometries and calculates the distance of each point along the flow line to the gully mouth (i.e., the outlet of the gully basin) (Fig. 5a).

The second part of the model includes first script (Fig. 5b) to make routing process for all the point along the flowline and to prepare the tables including the geographic coordinates (Easting and Northing values) and the elevation points from the initial digital elevation model along the flow line. This information will

be used later to embed the simulation results given as local coordinates into the DEM and thus the real-world spatial reference. The number of soil/substrate layers and their thicknesses can be added by the user in order to calculate the elevation of each layer along the point geometry. Finally, the third part of model is a script (Fig. 5c) to generate the topographic file including the flow accumulation as well as the elevation of each point and geographic coordinates along the surface of each layer in the form of a text file as input for the simulation.

## 4.3 Gully simulation

This step aims at the calculation of the main gully morphometry. The script computes for given time steps the main geometrical parameters of the area that is affected by gully erosion such as the change in incision depth, the change in top- and bottom width of each layer, which is represented by the point features along the gully flow line, as well as the volume of the gully erosion and the cross-sectional area along the flow lines. As input for the gully model runoff data and the soil parameters (critical velocity, slope stability, and erodibility coefficient) for each layer, as well as the topographic information from the step before are passed to the Python script.

Altogether four Python functions were used: 1) a function defining the calculation environment i.e., the input parameters such as time steps for the numerical solution of the differential equations as well as for the output interval, topographic parameters, runoff, and soil parameters; 2) a function implementing the numerical solution of the main equations based on Sidorchuk's model; 3) a function calculating the soil parameters such as slope stability, critical velocity, and erodibility coefficient for each point along the selected flow lines as well as the wall correction equation from the cuboid form to trapezoidal form; and, finally, 4) a function that writes the output parameters in respect to the defined interval.

## 4.4 Gully visualization

The last step regards the visualization of the model output in a GIS environment. The aim of this stage is to embed the calculated gully depths and widths values along the flow line into a coordinate system in order to be visualized in a 2D and/or a 3D visualization format, together with the related topography. This embedding is achieved by calculating 3D polygon features representing the gully bottom and the gully walls between adjacent flow line points for each time step, e.g., for each year. These polygons were created based on the defined coordinate file of the study area calculated in the data preparation step, and the geometrical parameters that were calculated in the simulation. Using simple geometric calculations implemented in a Python script, the local coordinates along the flow line for each layer are transformed into coordinates (Easting and Northing values) related to a geographic coordinate system. Additionally, the script creates 3D polygon geometries based on the GIS API for each year. The polygons can be projected and merged to define the upper boundary of gully erosion. As an output of this script, we achieve sequences of polygons that represent the bottoms and side walls of the stream flow lines for each layer after the erosion process of each time steps (e.g. yearly). The creation of these sequences of polygon geometries is used in the further 2D and 3D output visualization of gully erosion in the GIS environment.

## 5 Results And Discussion

Before starting the model processing steps, all relevant geo-data were projected in the spatial reference system UTM zone 35 South related to the geodetic datum WGS84. The flow lines have been extracted from the original DEM of the study area as shown in Fig. 6. The resulting flow lines were evaluated visually by overlaying the RGB orthomosaic of the study area. The extracted main flow line is coinciding with the main path of the gully development. Therefore, this main flow line was selected to calculate the gully's geometry. The model preparation step was run on the selected main flow line. This flow line was transformed into a sequence of point features. We assigned to each point the elevation of each soil or substrate layer, flow accumulation, and the coordinates of each point.

In the simulation step, different parameters were calculated such as the volume of gully erosion, the change of the cross-sectional area, and the change of the length of the gully corresponding to the number of years used in the simulation. During precipitation events, water runoff excavates a rectangular shaped channel cross-section in the topsoil or at the gully bottom. The incision is mainly dictated by the imbalance of detachment of particles from and the sedimentation on the gully bottom [37].

The model in the end allows the calculation of the final gully morphology. The mechanism of incision is mainly related to actual flow velocity that must be higher than the critical velocity for sedimentation. The shape of the longitudinal profile of the gully is decoupled from the initial slope and the evolution of the gully is controlled only by discharge parameters like critical velocity and soil texture.

Particularly, the critical velocity of the soils and substrates, as well as the extent of runoff discharge, primarily affect the speed of incision of the gully [39]. For the implemented model, the erosion rate of the first year was assumed to be of 0.5 m depth corresponding to the Solonetzic soil characteristics showing high erodibilities in the Btz horizon at 0.5m soil depth. Figure 7 shows that the length of the gully evolves very fast following the findings of Kosov et al. (1978) [17]. Already 80% of gully length is developed after ca. 20 years. The area values show an almost stable behavior after 60% of gully lifetime. Instead, the evolution of the gully depth and gully volume is much slower and continues up to the end of gully's lifetime.

In the last modelling step, the results are visualized in 2D and 3D visualizations utilizing a GIS environment (Fig. 8) As Sidorchuk (1999) [37] noted, during the dynamic phase of gully formation, runoff can be eroded a rectangular channel into the topsoil or gully floor. Thereafter, the vertical sidewalls of the gully may be unstable, resulting in small mass movements and further erosion. Hence, the rectangular cross-sections transform into a trapezoidal shape. In this stage, the simulation assumes straight alignment of finite elements for the flow line. However, the translation of the modelled flow line into the real flow line topography using the geographic coordinates is quite challenging for the visualization in an GIS environment due to curved bottom features and side wall characteristic.

The problem with the bending flow line was tackled by calculating line segments perpendicular to the flow line based on the modelled top width. Points with overlapping line segments were skipped in the

calculation. If the segments are not overlapping, the coordinates of the points defined by the top and bottom width of the layer are calculated as well as the coordinates of the points defining both side walls to the bottom of the respective layer. These points are used as vertices for polygons representing the boundaries of erosion areas for each time step (e.g. year). The width of the gully and the area of incision were simulated over a 50-years period. Both side walls of the primary water flow can be visualized in a 3D-view.

For a detailed validation of the results and for a sensitivity analysis of the model, different parameters were tested. Particularly, we tested the sensitivity of flow discharge and critical velocity over 50 years model runs, keeping constant all other model settings. Two discharge magnitudes were simulated just changing the units from l/s to m<sup>3</sup>/s corresponding to an increase by a factor of 1000. Concerning the critical velocity, we tested two different values representing two different soils: i) a resistive soil with high critical velocity (0.57 m/s) and ii) an erodible soil with low critical velocity (0.32 m/s). It was observed that discharge values have significant effect on gully area and volume evolution. The volume of the gully increases significantly with the increase of the discharge magnitude as shown in Fig. 9-A. Additionally, it has also been observed that the resistant soil with high critical velocity (0.57 m/s) has a lower total gully volume than the soft soil with low critical velocity (0.32 m/s). Consequently, the highest potential for gully erosion is close to the gully outlet since we have the largest discharge values (see Fig. 9-A). This may lead to incision for low resistive substrates or a broadening of the gully if resistive layers are reached as shown in Fig. 9-B. However, as shown the simulation model is very sensitive to changes of critical velocity and discharge; therefore, these parameters should be selected carefully.

## 6 Conclusion

Gully erosion is associated with a variety of on-site and off-site damages, particularly affecting agricultural lands. Government and research institutions around the world have been trying for years to evaluate the hazards associated with gully erosion and to predict their geographical distribution. The implemented code we present in this paper is mainly based on Sidorchuk's gully model using Python libraries along with GIS APIs. Thus, finally we propose a modelling tool implemented in a GIS environment to assess the changes in gully morphology over time. Hence, gully evolution over the full gully lifetime can be simulated. The application uses relevant input data of the study area such as the topographic characteristics, soil and substrate properties as well as surface runoff information. This data is preprocessed and organized to be easily implemented and visualized in the GIS environment. The application is designed to model annual changes in gully morphology. The complete simulation can be divided into four main steps: Step 1) establishment of the flow lines from a digital elevation model; Step 2) preparation of the topographic data relevant to select flow paths that represent gully erosion; Step 3) calculation of the main morphometric parameters such as length, width, depth, and volume per each segment along the flow path that finally allows for the calculation of soil erosion for each year; and Step 4) visualization of the main morphometric features and dynamics of gully erosion in a GIS.

The application is able to handle many different layers of soil or substrates. It must be noted that processing time depends on the number of flow lines, number of years for discharge data, and the erodibility coefficient of the soil layer types. The erodibility coefficient is used as a Courant number in the numerical solution of the underlying differential equations defining the internal time step. Thus, the higher the value the more time is needed to incise or erode a certain layer or to shape the bottom width of a gully channel. The quality of the generated model depends mainly on the input parameters e.g., soil characteristics, discharge data, and topographic data derived from DEM. The resulting morphology can be analyzed to evaluate the amount of soil loss per year.

The tool was tested for a gully system of the KwaThunzi area located in the upper Mkomazi River basin in KwaZulu Natal, South Africa. The results were very promising through the visualization of the time series of the gully's development. However, there are still challenges to be faced especially related to the use of empirical parameters in the model. Especially, critical velocity and discharge are two sensitive parameters that need a careful calibration. Additionally, the simulation algorithm assumes straight alignment of finite elements. Improvement of the algorithm should consider the bending of the real flow line. Finally, the application should be applied in different geographical regions and climatological conditions, so that a better understanding of the role of the input parameters may be achieved.

## Declarations

### Acknowledgments

The authors would like to thank profoundly Prof. Dr. Alexey Sidorchuk for providing the code of the gully models and his fundamental support and cooperation throughout the entire process of implementing the model and writing this paper. Moreover, the authors would like to thank the Department of Photogrammetry and Geoinformatics of Stuttgart University of Applied Sciences, the Department of Geography of University of Tübingen as well as the Department of Earth and Environmental Sciences of Pavia University for providing relevant data and support in conducting this study.

### Authorship Contribution

**Adel Omran** Model developer, Analysis, Writing, Editing; **Dietrich schröder** Model developer, Writing, Editing; **Christian Sommer** Data provider, field Work, Writing and Editing; **Volker Hochschild** Data provider, and Editing; **Michael Maerker** Writing, Editing and field Work

**Conflicts of interest** the authors declare that the research was conducted in the absence of any commercial or financial relationships that could be construed as a potential conflict of interest.

## References

1. Angileri SE, Conoscenti C, Hochschild V, Maerker M, Rotigliano E, Agnesi V, 2016 Water erosion susceptibility mapping by applying Stochastic Gradient Treeboost to the Imera Meridionale River

- Basin (Sicily, Italy). *Geomorphology* 262:61–76
2. Archibold OW, Levesque LMJ, de Boe DH, Aitken AE, Delanoy L (2003) Gully retreat in a semi-urban catchment in Saskatoon, Saskatchewan. *Appl Geogr* 23:261–279. DOI: 10.1016/j.apgeog.2003.08.005
  3. Baade J (1994) Gelände Experiment zur Verminderung des Schwebstoffes auf Kommen in landwirtschaftlichen Eizugsgebieten. PhD Thesis, University of Heidelberg
  4. Bogomolov AI, Mikhaylov KA (1972) *Hydravlica* Sroyizdat, Moskva in Russian
  5. Borrelli P, Robinson DA, Fleischer LR et al (2017) An assessment of the global impact of 21st century land use change on soil erosion. *Nat Commun* 8, 2013. <https://doi.org/10.1038/s41467-017-02142-7>
  6. Bosino A, Bernini A, Botha GA, Bonacina G, Pellegrini L, Omran A, Hochschild V, Sommer C, Maerker M 2021 Geomorphology of the upper Mkhomazi River basin, KwaZulu-Natal, South Africa, with emphasis on late Pleistocene colluvial deposits. *Journal of Maps*, 17:3,5–16, DOI: 10.1080/17445647.2020.1790435
  7. Botha GA, Temme AJAM, Singh RG (2016) Colluvial deposits and slope instability. In: Knight J, Grab SW (eds) *Quaternary Environmental Change in Southern Africa: Physical and Human Dimensions*. Cambridge University Press, Cambridge
  8. Bull LJ, Kirkby MJ (1997) Gully processes and modelling. *Prog Phys Geogr* 21(3):354–374
  9. Chaplot V, Giborie G, Marchand P, Valentin C (2005) Dynamic modelling for linear erosion intiation and development under climate and land-use changes in northen Laos. *CATENA* 63:318–328
  10. Conradie DCU (2012) South Africa's Climatic Zones: today, Tomorrow. International Green Building Conference and Exhibition, Sandton, South Africa
  11. Frankl A, Poesse J, Deckers J, Haile M, Nyssen J (2012) Gully head retreat rates in the semi-arid highlands of Northern Ethiopia. *Geomorphology*, pp 185–195
  12. Haan CT, Barfield BJ, Hayes JC (1994) *Design Hydrology and Sedimentology for Small Catchments*. Academic Press, London
  13. Haregeweyn N, Poesen J, Nyssen J, Govers G, Verstraeten G, De Vente, Deckers J, Moeyerso J, Haile M (2008a) Sediment yield variability Northern Ethiopia: a quantitative analysis of its controlling factors. *CATENA* 75:65–76
  14. Hayas A, Vanwalleghem T, Laguna A, Peña A, Giráldez JV 2017 Reconstructing long-term gully dynamics in Mediterranean areas. *Hydrol. Earth Syst. Sci.*, 21,235–249
  15. Ionita I (2006) Gully development in the Moldavian Plateau of Romania. *CATENA* 68(2–3):133–140
  16. Kroon FJ, Thorburn P, Schaffelke B, Whitten S (2016) Towards protecting the Great Barrier Reef from land-based pollution. *Glob Change Biol* 22(6):1985–2002. <https://doi.org/10.1111/gcb.13262>
  17. Kosov BF, Nikol'skaya II, Zorina YF (1978) Eksperimental'nyye issledovaniya ovragoobrazovaniya. In: Makkaveev, N.I. (Ed.), *Eksperimental'naya Geomorfologiya*, vol. 3. Izd. Mosk. Univ., Moskva, pp. 113–140. In Russian

18. Li Z, Zhang Y, Zhu Q, He Y, Yao W, 2015 Assessment of bank gully development and vegetation coverage on the Chinese Loess Plateau. *Geomorphology* 228:462–469
19. Maerker M (2001) Regionale Erosionsmodellierung unter Verwendung des Konzepts der Erosion Response Units (ERU) am Beispiel zweier Flusseinzugsgebiete im südlichen Afrika. PhD. [https://www.db-thueringen.de/servlets/MCRFileNodeServlet/dbt\\_derivate\\_00001093/Maerker\\_Disse.pdf](https://www.db-thueringen.de/servlets/MCRFileNodeServlet/dbt_derivate_00001093/Maerker_Disse.pdf)
20. Marker M, Florke M, Vassolo S, Alcamo JGP (2003) *Preliminary assessment of IPCC-SRES scenarios on future water resources using the WaterGAP 2 model. MODSIM 2003: international congress on modelling and simulation*, vols 1–4 – vol 1: natural systems, pt 1; vol 2: natural systems, pt 2; vol 3: socio-economic systems; vol 4: general systems. P.440–445
21. Maerker M, Bosino A, Scopesi C, Giordani P, Firpo M, Rellini I (2020) Assessment of calanchi and rill-interrill erosion susceptibility in northern Liguria, Italy: A case study using a probabilistic modelling framework. *Geoderma* 371:114367
22. Maerker M, Pelacani S, Schröder B, 2011 A functional entity approach to predict soil erosion processes in a small Plio-Pleistocene Mediterranean catchment in Northern Chianti, Italy. *Geomorphology* 125:530–540
23. Mirtskhulava Ts Ye (1988) *Osnovy Fiziki i Mekhaniki Eroзии Rusel (Principles of physics and mechanics of channel erosion)* (in Russian). Gidrometeoizdat, Leningrad
24. Mitsova H, Barton M, Ullah I, Hofierka J, Harmon RS 2013 GIS-based soil erosion modeling. In: Shroder, J. (Editor in Chief), Bishop, M.P. (Ed.), *Treatise on Geomorphology*. Academic Press, San Diego, CA, vol. 3, Remote Sensing and GIScience in Geomorphology, pp. 228–258. DOI: 10.1016/B978-0-12-374739-6.00052-X
25. Nel W (2009) Rainfall trends in the KwaZulu-Natal Drakensberg region of South Africa during the twentieth century. *Int J Climatol* 29:1634–1641
26. Omran A, Dietrich S, Abouelmagd A, Michael M (2016) New ArcGIS tools developed for stream network extraction and basin delineations using Python and java script. *Comput Geosci* 94:140–149
27. Park Y, Kim J, Engel B et al (2009) Development of web-based SWAT System. *Proceedings of ASABE*, Reno, Nevada
28. Partridge TC, Dollar ESJ, Moolman J, Dollar LH (2010) The geomorphic provinces of South Africa, Lesotho and Swaziland: A physiographic subdivision for earth and environmental scientists. *Trans Royal Soc South Afr* 65:1–47
29. Poesen J, Govers G (1990) Gully erosion in the loam belt of Belgium: typology and control measures. In: *Soil Erosion on Agriculture land* (ed. By J. Boardmann, I. D. L. Foster & J. A. Dearing), 513–530. Wiley, Chichester, UK
30. Poesen JWA, Torri DB, Van Walleghem T (2011) Gully erosion: procedures to adopt when modelling soil erosion in landscapes affected by gullying. In: Morgan RPC, Nearing MA (eds) *Handbook of Erosion Modelling*. Oxford, Blackwell, pp 360–386

31. Poesen J, Vandaele K, van Wesemael B Gully erosion: importance and model implications. In Boardman J, Favis-Mortlock DT (eds), *Modelling Soil Erosion by Water*. Springer-Verlag, Berlin Heidelberg, NATO-ASI Series(1998) I-55:285–311
32. Poeter E, Hill M, Banta E, Mehl S, Christensen S 2005 UCODE 2005 and six other computer codes for Universal Sensitivity Analysis, calibration, and uncertainty evaluation, technical report, USGS
33. Renard KG, Foster GR, Weesies GA, McCool DK, Yoder DC(1997) Predicting soil erosion by water: a guide to conservation planning with the Revised Universal Soil Loss Equation (RUSLE). *Agriculture Handbook No. 703*, USDA-ARS
34. Schaller J, Gehrke T, Strout N (2009) ArcGIS Processing Models for Regional Environmental Planning in Bavaria. In: Geertman S, Stillwell J (eds) *Planning Support Systems Best Practice and New Methods*. The GeoJournal Library, vol 95. Springer, Dordrecht. [https://doi.org/10.1007/978-1-4020-8952-7\\_13](https://doi.org/10.1007/978-1-4020-8952-7_13)
35. Schröder D, Omran A (2013) Terrain analysis for flash flood risk mapping. In: *Proceeding of Applied Geoinformatics for Society and Environment (AGSE)*, HFT-Stuttgart, Germany. p. p.1–8. ISBN978-3-940670-42-2
36. Sidorchuk A (1996) Gully erosion and thermo-erosion on the Yamal Peninsula. In: *Geomorphic Hazards* (ed. by O. Slaymaker), 153–168. John Wiley, New York
37. Sidorchuk A (1999) Dynamic and static models of gully erosion. *Catena Vol 37:3–4*
38. Sidorchuk A (2021) Models of Gully Erosion by Water. *Water 13:3293*. <https://doi.org/10.3390/w13223293>
39. Sidorchuk A, Maerker M, Moretti S, Rodolfi G (2001) Soil erosion modelling in the mbuluzi river catchment (swaziland, south africa). part i: Modelling the dynamic evolution of gullies. *Geografia Fisica e Dinamica Quaternaria*. Vol. 24, no. 2. – P. 177–187
40. Sidorchuk A, Maerker M, Moretti S, Rodolfi G (2003) Gully erosion modelling and landscape response in the Mbuluzi River catchment of Swaziland. *CATENA 50:507–525*
41. Sidorchuk A, Sidorchuk A (1998) Model for estimating gully morphology. *IAHS Publ 249:333–343* (Wallingford)
42. Torri D, Poesen J, Rossi M, Amici V, Spennacchi D, Cremer C (2018) Gully head modelling: A Mediterranean badland case study. *Earth Surface Process and Landforms*, Wiley, 43, <https://doi.org/10.1002/esp.4414>
43. Trofimov A, Moskovikin VM 1983 *Metamaticheskoye Modelirovaniye v Geomorfologii sklonov* (mathematical modelling in geomorphology of slopes). IZd. Kazan Univ., Kazan
44. US Soil Conservation Service (1966) *Procedures for Determining Rates of Land Damage, Land Depreciation and Volume of Sediment Produced by Gully Erosion*. Tech. Release no. 32, US Dept Agric, Washington
45. Vandekerckhove L, Muys B, Poesen J, Weerdt BD, Coppe N 2001 A method for dendrochronological assessment of medium-term gully erosion rates. *Catena*, 45,123–161

46. Vanmaercke M, Panagos P, Vanwalleghem T et al 2021 Measuring, modelling and managing gully erosion at large scales: A state of the art, *Earth-Science Reviews*  
<https://doi.org/10.1016/j.earscirev.2021.103637>
47. Wesseling CG, Karssenberg D, Van Deursen WPA, Burrough PA (1996) Integrating dynamic environmental models in GIS: the development of a dynamic modelling language. *Trans GIS* 1:40–48
48. Zabihi M, Mirchooli F, Motevalli A, Darvishan AK, Pourghasemi HR, Zakeri MA, Sadighi, F 2018 Spatial modelling of gully erosion in Mazandaran Province, northern Iran. *Catena*, 161,1–13
49. Zorina F (1979) Raschetnyye method opredeleniya potentsiala ovrazhnoy erozii (Methods of calculating gully erosion potential). *Eroziya pochv I Ruslovyye Protsessy (Soil erosion and channel process)* (in Russian), vol 7. Univ. Press, Moscow, pp 81–90.

## Figures

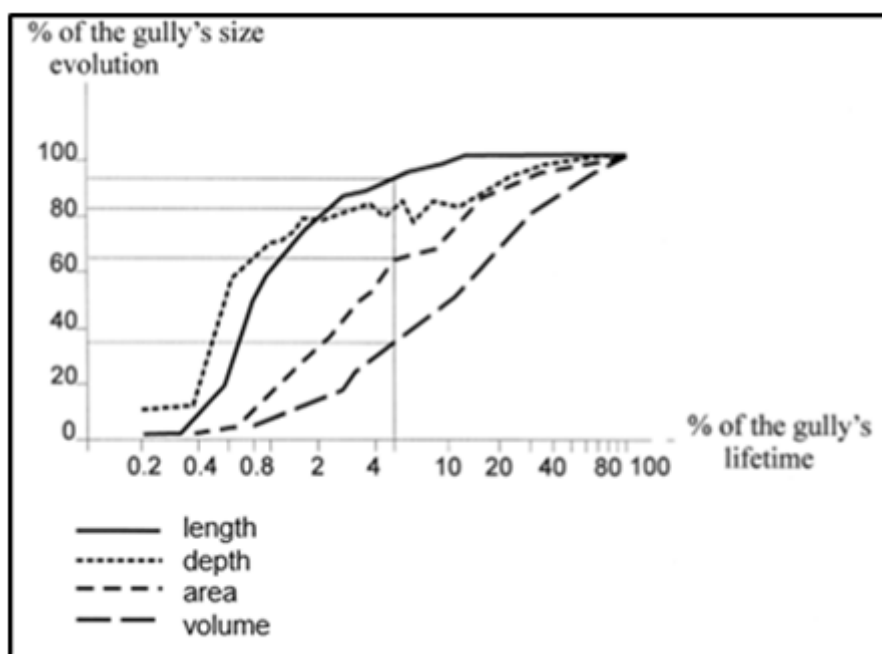


Figure 1

Evolution of the gully morphology through time: after Kosov et al., 1978 [17]

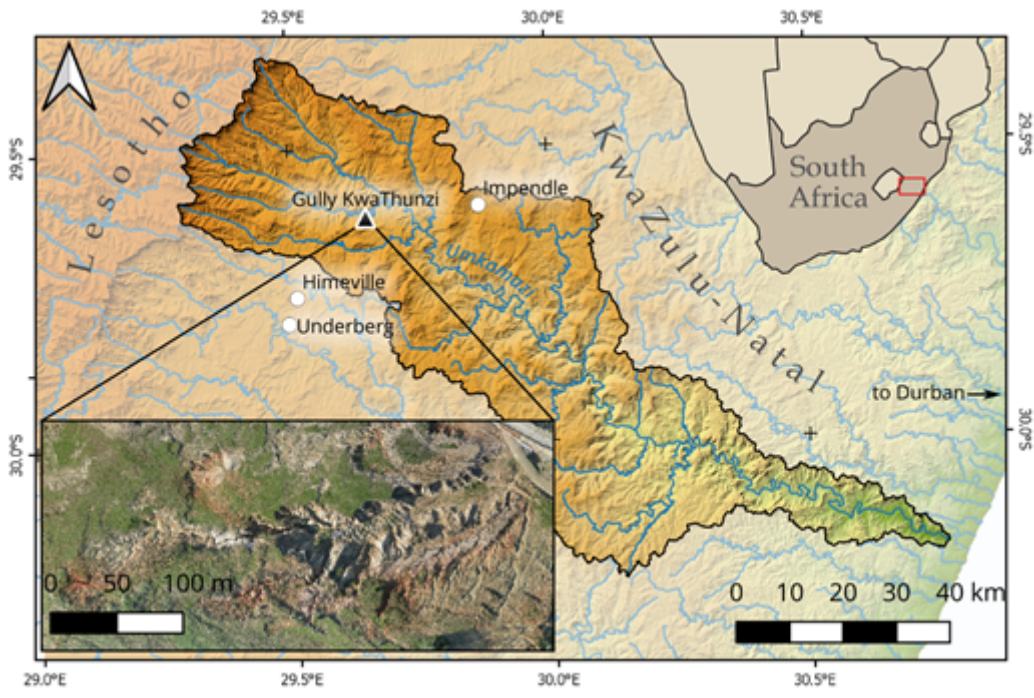


Figure 2

Location of the gully Kwa Thunzi – South Africa

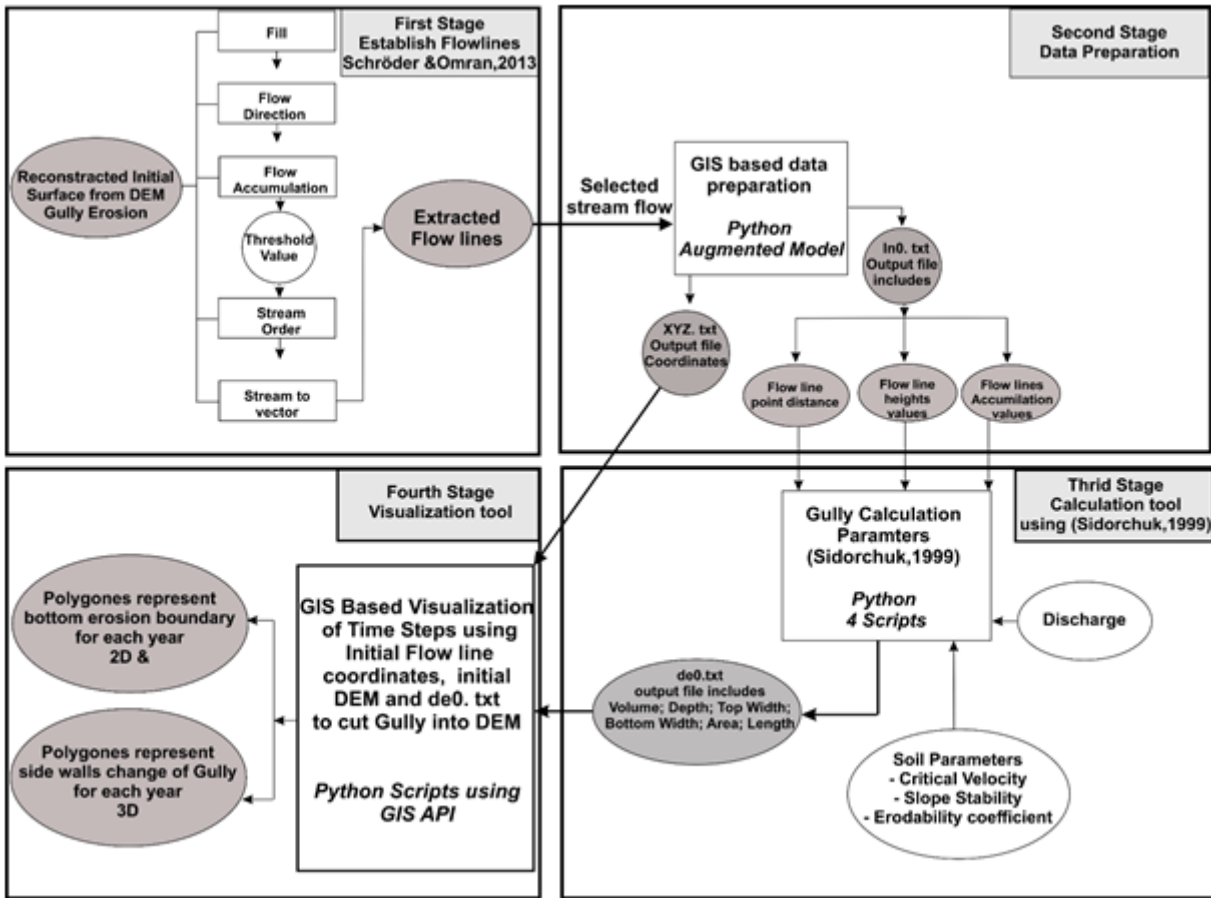


Figure 3

Workflow Scheme of the GIS Model of Gully Erosion

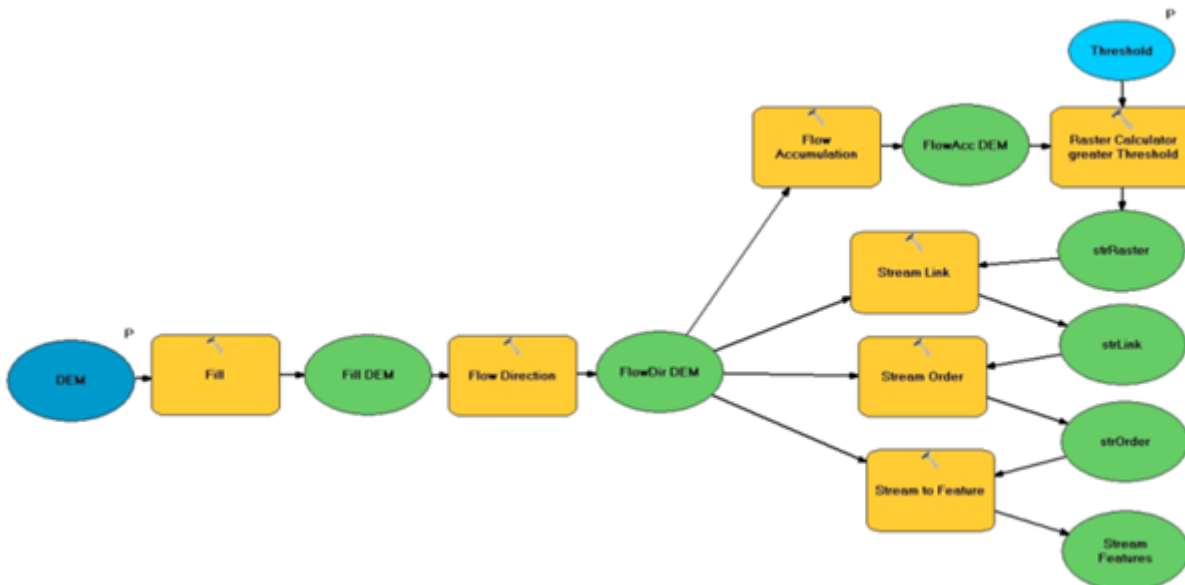


Figure 4

Automated stream network extraction using the GIS Model [35]

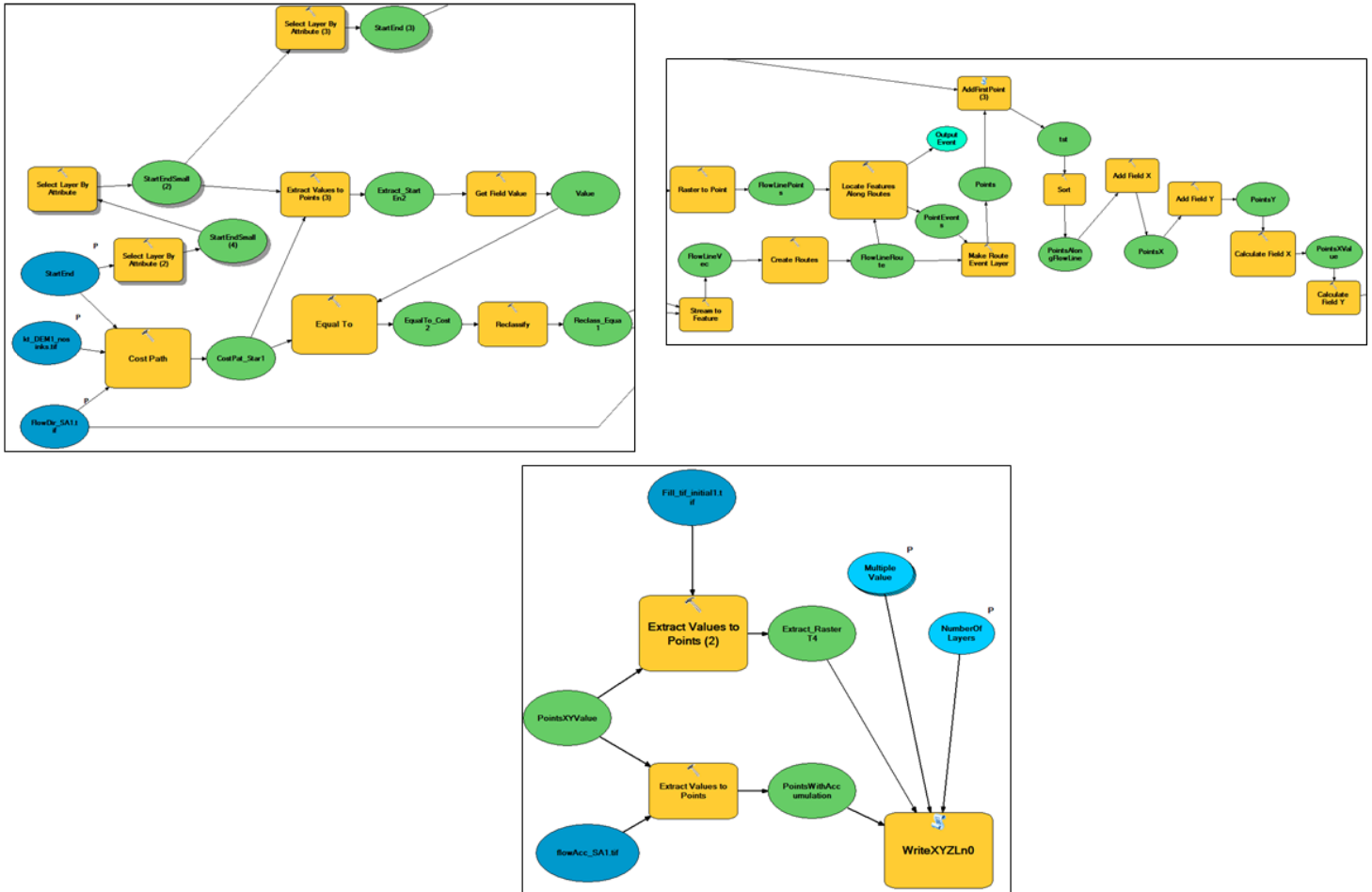


Figure 5

a: Procedure to convert flowlines to points and attributing flow accumulation

b: Procedure for routing process and extracting the input table: Procedure extracting the coordinates of flow line points

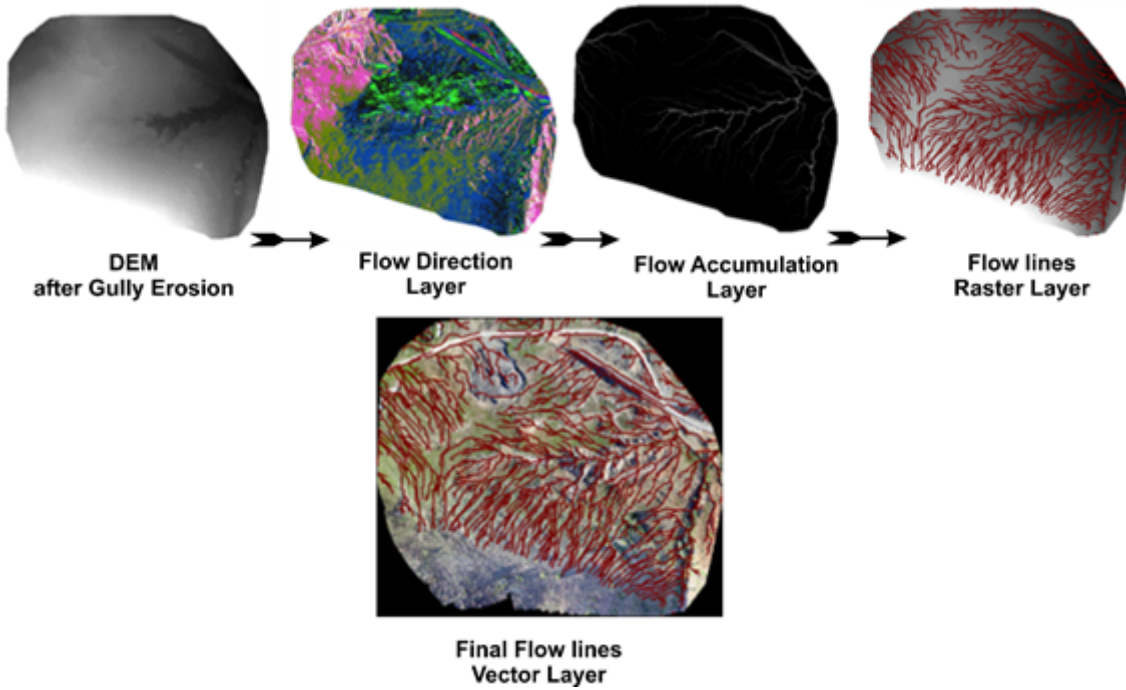


Figure 6

Extraction of streamflow lines from high resolution DEM (15 cm)

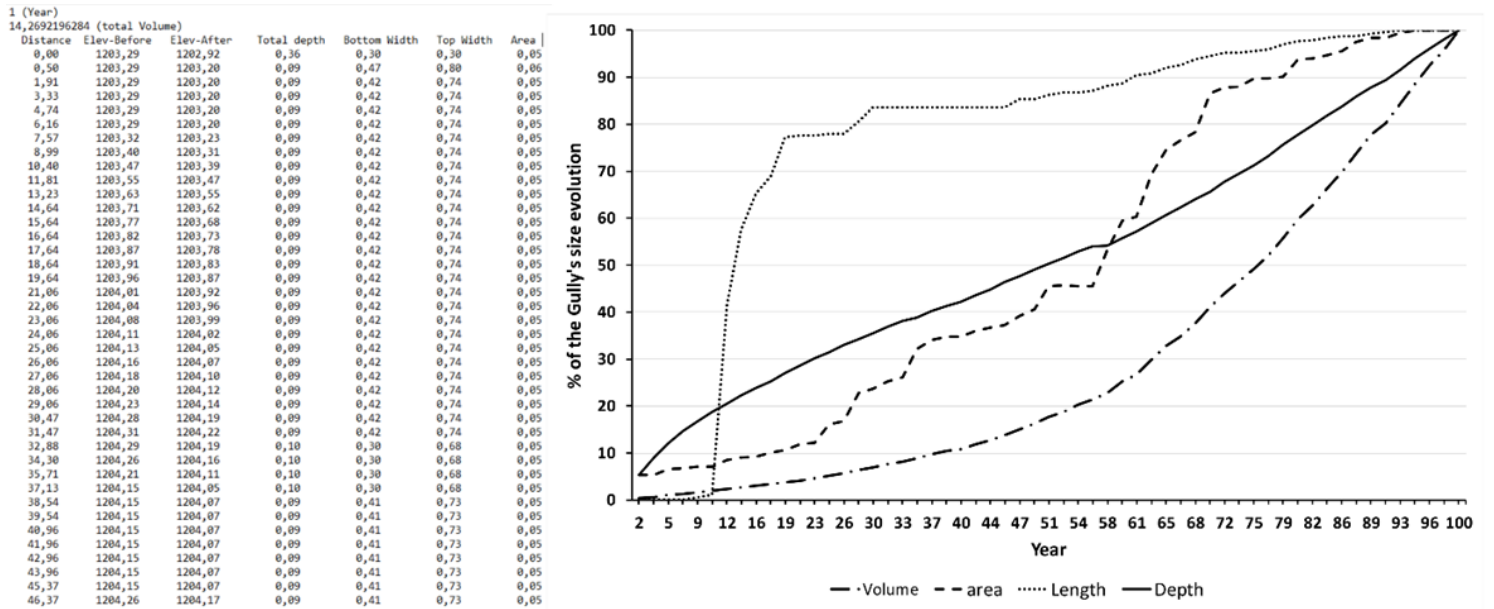


Figure 7

The results of the simulation step, the left side represents the text files of the calculated parameters for gully erosion (total depth, total volume, change in top width, change in bottom width, and the change in area for each year) and the right side represents the changes of gully in volume, length, depth, and area over time.

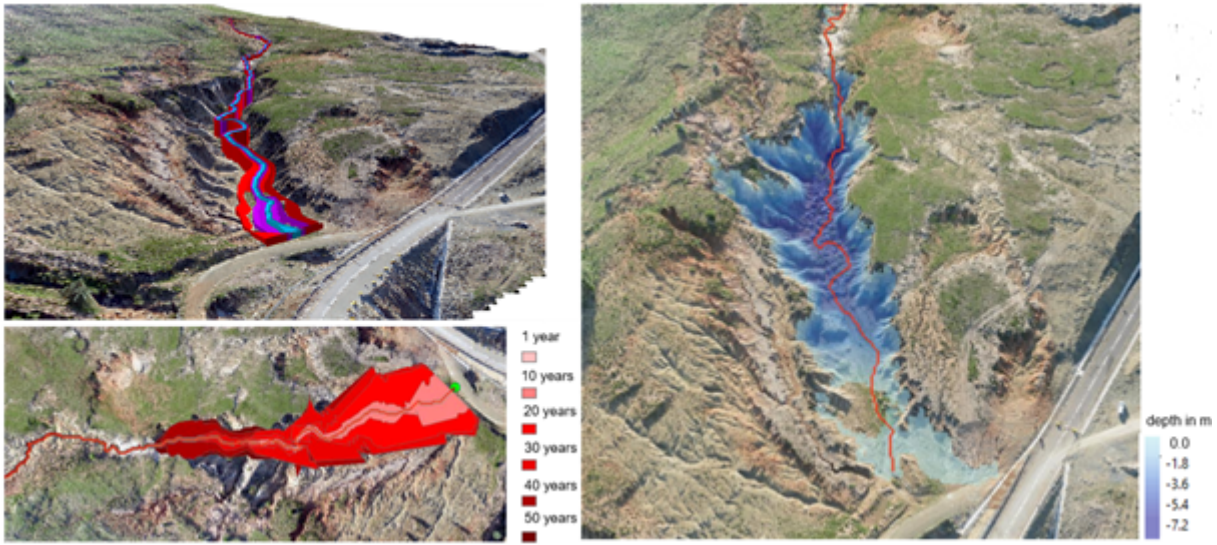


Figure 8

Simulated Gully bottom evolution during a 50-year period – 2D and 3D view



Figure 9

a: Effect of changed discharge units on gully erosion.

b: Effect of the changed critical velocity values on gully erosion.